NON-ITERATIVE SOLVERS FOR NONLINEAR PROBLEMS: THE CASE OF COLLISIONS

Michele Ducceschi *

Acoustics and Audio Group
University of Edinburgh
Edinburgh, UK
michele.ducceschi@ed.ac.uk

Stefan Bilbao

Acoustics and Audio Group
University of Edinburgh
Edinburgh, UK
s.bilbao@ed.ac.uk

ABSTRACT

Nonlinearity is a key feature in musical instruments and electronic circuits alike, and thus in simulation, for the purposes of physics-based modeling and virtual analog emulation, the numerical solution of nonlinear differential equations is unavoidable. Ensuring numerical stability is thus a major consideration. In general, one may construct implicit schemes using well-known discretisation methods such as the trapezoid rule, requiring computationally-costly iterative solvers at each time step. Here, a novel family of provably numerically stable time-stepping schemes is presented, avoiding the need for iterative solvers, and thus of greatly reduced computational cost. An application to the case of the collision interaction in musical instrument modeling is detailed.

1. INTRODUCTION

Computer simulation of physical systems is at the core of many disciplines, and physical modeling sound synthesis is no exception. The scope of research into physical modeling has expanded to include the simulation of very complex musical systems, including lumped as well as fully-distributed nonlinearities; musically, many perceptually important phenomena can be viewed as originating from this nonlinear behaviour. A specialised approach is often required at the simulation stage, particularly in ensuring numerical stability—a major concern in the modeling of systems with strong nonlinearities. One approach to the design of numerically-stable schemes is through the use of energy methods. With rare exceptions, however, such designs require the use of iterative numerical schemes, thus increasing computational costs.

Recently, non-iterative numerical integrators for a class of nonlinear ordinary differential equations have been devised through the port-Hamiltonian approach for virtual-analog simulations [1, 2, 3]. The schemes employ a suitable quadratisation of the nonlinear potential [4] which gives, ultimately, an update which can be performed without the use of an iterative method such as, e.g., Newton-Raphson.

In the current work, the possibility of using non-iterative solvers for nonlinear problems is developed further, to the case of a non-invertible potential, and for fully distributed systems described by partial differential equations (PDEs). The focus here will be on collisions, a topic of longstanding attraction for researchers in physical modeling sound synthesis [5, 6, 7, 8, 9, 10, 11, 12, 13]. Collisions here serve as useful and practically important test case, because the method can be applied in the current form to any second-order-in-time system with a non-negative potential energy, and can be extended to higher-order systems. The current method leads to significant speedups, in some cases of one order of magnitude, see [14]. Moreover, with respect to iterative methods, existence and uniqueness of the numerical solution are proven trivially by inspection of the update equation.

The method is described in detail in Section 2. There, an overview is given, along with a numerical experiment dealing with a mass-spring system colliding against a barrier. In Section 3, a case of interest in musical acoustics is studied, i.e. the collision of a musical string against a distributed barrier. Iterative schemes, developed in previous works, are used for bench marking. Novel non-iterative finite difference schemes and modal schemes are developed, showing convergence of all the methods to a common solution. Stability is proven mathematically by energy arguments, and illustrated in a number of numerical experiments.

2. PRELIMINARIES

Before examining a fully distributed system, it is useful to explore the method in the case of a typical lumped system in a mechanical setting, described by a single time-dependent ordinary differential equation (ODE):

$$M\ddot{u} + \phi'(u) = 0 \tag{1}$$

Here, $u = u(t)$ is a displacement of a lumped object of mass M, and as a function of time t. Dots represent derivatives with respect to t. $\phi = \phi(u)$ is a function representing the potential energy of the system, and $\phi' = d\phi/du$. (Note that if $\phi(u) = Bu^2/2$, for some constant $B > 0$, then (1) represents the equation of motion of a simple harmonic oscillator.)

Using the chain rule, it is possible to rewrite (1) as

$$M\ddot{u} + \dot{\phi}/\dot{u} = 0 \tag{2}$$

Conservation of energy may be achieved by directly multiplying both sides of (2) by $\dot{u}$, yielding

$$\frac{d}{dt}\underbrace{\left(\frac{M\dot{u}^2}{2} + \phi\right)}_{\triangleq H(t)} = 0 \tag{3}$$

and hence

$$H(t) = H(0) \triangleq H_0. \tag{4}$$

Non-negativity of the potential energy ϕ reflects a condition for passivity of (1). Under such a condition, the total conserved energy H_0 is non-negative, and one may bound the growth of the state as

$$0 \leq |\dot{u}| \leq \sqrt{2H_0/M} \tag{5}$$

* The author's work was supported by the Leverhulme Trust with an Early Career Fellowship

More restrictive conditions on ϕ (such as radial unboundedness) allow for global asymptotic stability, but the above non-negativity condition will suffice for the present purposes, and allows physically-reasonable solution growth (i.e., inertial drift).

The new schemes proposed in this work are based on an equivalent expression for (1):

$$M\ddot{u} + \psi\psi' = 0 \qquad \text{with} \qquad \psi = \sqrt{2\phi} \tag{6}$$

By means of the chain rule, (6) may be written as

$$M\ddot{u} + \psi\left(\dot{\psi}/\dot{u}\right) = 0 \tag{7}$$

and energy conservation is obtained by multiplication by $\dot{u}$, on both sides, yielding

$$\frac{d}{dt}\underbrace{\left(\frac{M\dot{u}^2}{2} + \frac{\psi^2}{2}\right)}_{\triangleq H(t)} = 0 \tag{8}$$

This form of the energy function is analogous to the form given in [3] developed within the Port-Hamiltonian framework. Clearly, (8) is equivalent to (3), given the definition in (6). Hence, (7) is equivalent to (2), and bounds (5) hold.

Passivity and equivalence of (7) and (2) are possible only under non-negativity of the potential ϕ—an entirely natural requirement. Though various forms of the potential appear in musical acoustics, here, one particular form will be explored, namely:

$$\phi(\eta) = \frac{K}{(\alpha+1)}[\eta]_+^{\alpha+1}, \quad K \geq 0,\ \alpha \geq 1 \tag{9}$$

where $[\eta]_+ \triangleq 0.5(\eta + |\eta|)$ is the *positive part* of η. This potential is clearly non-negative. It has been employed as a penalty-potential in collision models in musical acoustics [15, 8], and it is derived from Hertz's contact law.

2.1. Linear Oscillator With Barrier

In preparation to the fully distributed case, (1) is now equipped with a linear restoring force. Hence

$$M\ddot{u} = -\phi'(\eta) - M\omega_0^2 u \tag{10}$$

with ϕ given by (9), and where

$$\eta = u - b \tag{11}$$

This model describes a mass-spring system, with linear radian frequency $\omega_0 = 2\pi f_0$, with f_0 measured in Hz, colliding from below against a barrier placed at b. This differential equation can be cast in the two equivalent forms, as seen above. These are

$$M\ddot{u} = -\dot{\phi}/\dot{\eta} - M\omega_0^2 u \tag{12a}$$

$$M\ddot{u} = -\psi\left(\dot{\psi}/\dot{\eta}\right) - M\omega_0^2 u \tag{12b}$$

Energy conservation for the above equations reads, respectively,

$$\frac{d}{dt}\left(\frac{M\dot{u}^2}{2} + \frac{M\omega_0^2 u^2}{2} + \phi\right) = 0 \tag{13a}$$

$$\frac{d}{dt}\left(\frac{M\dot{u}^2}{2} + \frac{M\omega_0^2 u^2}{2} + \frac{\psi^2}{2}\right) = 0 \tag{13b}$$

and thus the same bounds as (5) hold in both cases.

2.2. Time Difference Operators

Solutions to (12a) and (12b) are sought by means of appropriate finite difference schemes. Time is discretised by means of a sample rate f_s, yielding a time step $k = 1/f_s$. u^n represents an approximation to the continuous function $u(t)$ at time $t = nk$, for integer n. Finite time difference operators are now introduced.

The identity and temporal shift operators are defined as

$$1u^n = u^n, \quad e_{t+}u^n = u^{n+1}, \quad e_{t-}u^n = u^{n-1} \tag{14}$$

Notice that the similar definitions hold for operators acting on interleaved grid functions [16], as in

$$e_{t+}\psi^{n-1/2} = \psi^{n+1/2}, \quad e_{t-}\psi^{n+1/2} = \psi^{n-1/2} \tag{15}$$

From these, it is possible to define the forward, backward and centred time differences, all approximating a first time derivative, as

$$\delta_{t+} = \frac{e_{t+} - 1}{k}, \quad \delta_{t-} = \frac{1 - e_{t-}}{k}, \quad \delta_{t\cdot} = \frac{e_{t+} - e_{t-}}{2k} \tag{16}$$

An approximation to the second time derivative is constructed by composition of the operators presented above, as

$$\delta_{tt} = \delta_{t+}\delta_{t-} \tag{17}$$

Finally, forward and backward averaging operators may be defined as

$$\mu_{t+} = \frac{e_{t+} + 1}{2}, \quad \mu_{t-} = \frac{1 + e_{t-}}{2} \tag{18}$$

2.2.1. Iterative Conservative Finite Difference Scheme

Following the derivation in [8], a suitable discretisation of (12a) is

$$M\delta_{tt}u^n = -M\omega_0^2 u^n - \frac{\delta_{t+}\phi^{n-1/2}}{\delta_{t\cdot}\eta^n} \tag{19}$$

where

$$\phi^{n-1/2} \triangleq \mu_{t-}\phi(\underbrace{u^n - b}_{\eta^n}) \tag{20}$$

Stability of the scheme may be inferred from energy analysis, after multiplication of both sides of (19) by $\delta_{t\cdot}u^n$. This gives

$$\delta_{t+}\left(\underbrace{\frac{M(\delta_{t-}u^n)^2}{2} + \frac{M\omega_0^2 u^n u^{n-1}}{2} + \phi^{n-1/2}}_{\mathfrak{H}^{n-1/2}}\right) = 0$$

This is clearly a discrete counterpart of (13a). In this case, the non-negativity of the total energy can be assured if and only if [16]

$$\omega_0 < 2f_s \tag{21}$$

Under such condition, one may write

$$0 \leq |\delta_{t-}u^n| \leq \sqrt{2\mathfrak{H}^{1/2}/M} \tag{22}$$

and hence the boundedness of the state follows. Scheme (19) can be written as

$$\underbrace{r - 2u^n + 2u^{n-1} + k^2\omega_0^2 u^n + \frac{k^2}{M}\frac{\phi(r+a) - \phi(a)}{r}}_{G(r)} = 0, \tag{23}$$

where

$$r \triangleq u^{n+1} - u^{n-1}, \quad a \triangleq b - u^{n-1}.$$

Because the unknown r appears implicitly as the argument of ϕ, an iterative root finder (such as Newton-Raphson) must be employed in order to solve $G(r) = 0$ as per (23). The solution to the scheme can be shown to be unique — see [13, 8].

2.2.2. Non-iterative Conservative Finite Difference Scheme

A novel, non-iterative finite difference scheme follows as a suitable discretisation of (12b), as

$$M\delta_{tt}u^n = -M\omega_0^2 u^n - \left(\mu_{t+}\psi^{n-1/2}\right)\frac{\delta_{t+}\psi^{n-1/2}}{\delta_{t\cdot}\eta^n} \tag{24}$$

This may be rewritten as the following system:

$$M\delta_{tt}u^n = -M\omega_0^2 u^n - \left(\mu_{t+}\psi^{n-1/2}\right) g^n \tag{25a}$$

$$\delta_{t+}\psi^{n-1/2} = g^n \delta_{t\cdot}\eta^n \tag{25b}$$

where g^n may be explicitly computed as

$$g^n = \psi'\Big|_{\eta=\eta^n} = \frac{\phi'}{\sqrt{2\phi}}\Big|_{\eta=\eta^n} \tag{26}$$

Here, we may use the analytic expressions for ψ and ϕ directly in the computation of g^n. Stability of the scheme can be deduced from an energy conservation law, obtained after multiplication of (24) by $\delta_{t\cdot}u^n$. Energy is thus conserved according to

$$\delta_{t+}\left(\underbrace{\frac{M(\delta_{t-}u^n)^2}{2} + \frac{M\omega_0^2 u^n u^{n-1}}{2} + \frac{(\psi^{n-1/2})^2}{2}}_{\mathfrak{H}^{n-1/2}}\right) = 0$$

Inspection of the energy function allows to infer the same stability condition as (21). Thus, the same bounds as (22) hold in this case. Using the identity

$$\mu_{t+}\psi^{n-1/2} = \frac{k}{2}\delta_{t+}\psi^{n-1/2} + \psi^{n-1/2} \tag{27}$$

one may insert the value of $\delta_{t+}\psi^{n-1/2}$ from (25b) into (25a), to get

$$Au^{n+1} = v \tag{28}$$

where

$$A = \frac{M}{k^2} + \frac{(g^n)^2}{4}$$

$$v = \frac{M}{k^2}(2u^n - u^{n-1}) - M\omega_0^2 u^n + \frac{(g^n)^2}{4}u^{n-1} - \psi^{n-1/2}g^n$$

This scheme can thus be solved by division, and once u^{n+1} is computed, from (25a), one can update $\psi^{n+1/2}$ using (25b).

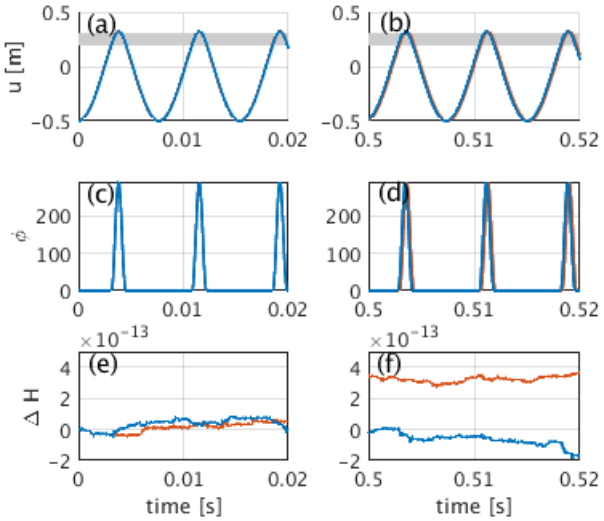

Figure 1: For all panels, the red line is the solution obtained via the iterative scheme (with 20 iterations), and the blue line is the solution obtained via the new scheme. A particle of mass $M = 10$g is launched with initial speed $v_0 = 1$m/s from $u_0 = -0.5$m against a rigid barrier with $\alpha = 1.1$, $K = 5 \cdot 10^4$, located at $b = 0.2$m. The particle is subjected to a linear restoring potential of frequency $f_0 = 10$Hz. The sample rate is chosen as $f_s = 44100$Hz. (a)-(b): displacement vs time, at times indicated. (c)-(d): potential ϕ, at times indicated. (e)-(f): energy variation $\Delta H = (\mathfrak{H}^{n-1/2} - \mathfrak{H}^{1/2})/\mathfrak{H}^{1/2}$, at times indicated.

2.3. Numerical Examples

The finite difference schemes given above are now compared in cases of practical use. In particular, two barriers with different stiffness constants are considered here. Fig. 1 depicts the case with a softer barrier. From panels (a)-(b), it is seen that the two schemes yield a converged solution for a long period of time. The value of the potential ϕ, visible in panels (c)-(d) is also the same over the same period. Finally, panels (e)-(f) show the variation of the total energy.

Fig. 2 considers the same oscillator, with a harder barrier. In this case, the two schemes yield a different solution. For the non-iterative scheme, the excess kinetic energy is converted to potential energy, so to guarantee energy conservation overall, keeping the scheme stable within the bounds (22), as visible in Fig.2(c)-(d). This is reflected in lower-than-expected collision output velocities. The variation of the total energy for the two schemes is visible in Fig.2(e)-(f). As expected, increasing the sample rate yields a converged solution, as can be seen in Fig. (3).

3. DISTRIBUTED SYSTEMS

In this section, the model schemes illustrated in the previous section are applied to cases of interest in musical acoustics, for advanced sound synthesis of string instruments. The system under study is composed of a taut string with stiffness, and of a rigid barrier. The motion of the string, of length L, can be described by

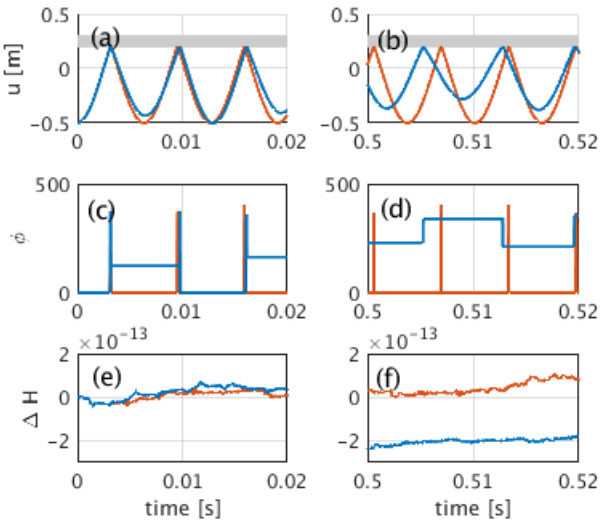

Figure 2: Same as Fig. 1, but with $K = 7 \cdot 10^7$.

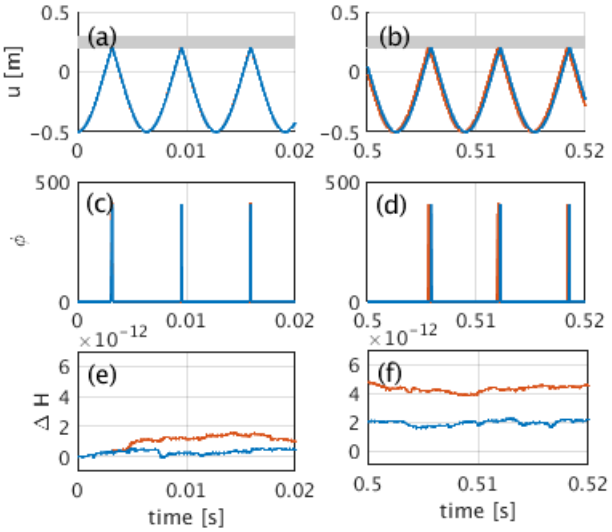

Figure 3: Same as Fig. 2, but with $f_s = 5 \cdot 44100$Hz

either one of the following equivalent equations

$$\rho\partial_t^2 u = \partial_x^2 T_0 u - \partial_x^4 EIu + \frac{\partial_t \phi}{\partial_t \eta} + \delta(x - x_F)F(t) \tag{29a}$$

$$\rho\partial_t^2 u = \partial_x^2 T_0 u - \partial_x^4 EIu + \psi\frac{\partial_t \psi}{\partial_t \eta} + \delta(x - x_F)F(t) \tag{29b}$$

where again

$$\psi = \sqrt{2\phi} \tag{30}$$

In the equations, $u = u(x,t)$ is the displacement of the string, now a function of both time and space. Notice that, having to deal with partial differentiation, the notation for derivatives has changed compared to the lumped case. The string is defined over $\mathcal{D} : x \in [0, L]$. Constants appear as: ρ, the linear density; T_0, the applied tension; E, Young's modulus; I, the moment of inertia of the cross section. The potential ϕ has now units of potential energy per unit length (i.e. energy density) , but its formal definition is again of the form (9), where

$$\eta = b - u \tag{31}$$

In the above, $b = b(x)$ is the height of barrier, supposed unmovable. Finally, $\delta(x - x_F)$ is a Dirac delta function. $F(t)$ will be here expressed as a raised cosine function, i.e.

$$F(t) = \begin{cases} \frac{F_0}{2}\left(1 - \cos\left(\frac{2\pi(t-t_0)}{t_{wid}}\right)\right), & t_0 \le t \le t_0 + t_{wid} \\ 0, & \text{otherwise} \end{cases}.$$

where F_0 and t_{wid} are input parameters controlling, respectively, the maximum amplitude of the forcing, and the contact duration, and t_0 is the activation time.

An inner product of two functions f, g, and the associated norm, are defined as

$$\langle f, g\rangle_{\mathcal{D}} \triangleq \int_0^L f\, g\, dx, \quad \|f\|_{\mathcal{D}}^2 \triangleq \langle f, f\rangle_{\mathcal{D}} \tag{32}$$

Under unforced conditions, i.e. for $F(t) = 0$, energy conservation and boundary conditions can be extracted after taking an inner product of (29a) and (29b) with $\partial_t u$. This gives, respectively,

$$\frac{d}{dt}\left(\underbrace{\frac{\rho\|\partial_t u\|_{\mathcal{D}}^2}{2} + \frac{T_0\|\partial_x u\|_{\mathcal{D}}^2}{2} + \frac{EI\|\partial_x^2 u\|_{\mathcal{D}}^2}{2} + \langle\phi, 1\rangle_{\mathcal{D}}}_{H(t)}\right) = 0 \tag{33a}$$

$$\frac{d}{dt}\left(\underbrace{\frac{\rho\|\partial_t u\|_{\mathcal{D}}^2}{2} + \frac{T_0\|\partial_x u\|_{\mathcal{D}}^2}{2} + \frac{EI\|\partial_x^2 u\|_{\mathcal{D}}^2}{2} + \frac{\|\psi\|_{\mathcal{D}}^2}{2}}_{H(t)}\right) = 0 \tag{33b}$$

where the identities above hold only under a choice of appropriate boundary conditions. Here, conditions of the *simply-supported* kind are enforced, hence

$$u = \partial_x^2 u = 0 \quad \text{at } x = 0, L \tag{34}$$

Given the non-negativity of the energy functions above, one may bound the norm of the state, as

$$0 \le \|\partial_t u\|_{\mathcal{D}} \le \sqrt{2H_0/\rho} \tag{35}$$

where H_0 is the value of the conserved energy (i.e. its initial value).

3.1. Iterative and Non-Iterative Finite Difference Schemes

Finite difference schemes are now constructed for the solution of (29a), (29b). Hence, both time and space are discretised along appropriate grids, and the grid function u_m^n is regarded as an approximation to the solution $u(x,t)$ at the time nk, and at mh, where k is the time step, h is the grid spacing, and m and n are integers. Time difference operators appear as in Section 2.2. Spatial

difference operators have analogous definitions, and hence

$$1u_m^n = u_m^n, \quad e_{x+}u_m^n = u_{m+1}^n, \quad e_{x-}u_m^n = u_{m-1}^n \tag{36}$$

From these, it is possible to define the forward and backward spatial differences, as

$$\delta_{x+} = \frac{e_{x+} - 1}{h}, \quad \delta_{x-} = \frac{1 - e_{x-}}{h} \tag{37}$$

Approximations to the second and fourth spatial differences are constructed from the above, as

$$\delta_{xx} = \delta_{x+}\delta_{x-}, \quad \delta_{xxxx} = \delta_{xx}\delta_{xx} \tag{38}$$

The spatial grid is defined for $\mathbb{M} : m \in \{0, 1..., M\}$. Sets of points lacking at least one end point will also be used: they are $\underline{\mathbb{M}} : m \in \{0..., M-1\}$, and $\overline{\mathbb{M}} : m \in \{1..., M-1\}$. A discrete version of (32), the inner product and associated norm, can be realised using summation. Hence

$$\langle f, g \rangle_{\mathbb{B}} \triangleq \sum_{b \in \mathbb{B}} h\, f_b^n\, g_b^n, \quad \|f\|_{\mathbb{B}}^2 \triangleq \langle u, u \rangle_{\mathbb{B}} \tag{39}$$

Finally, $\delta(x - x_F)$ is approximated by a zeroth-order spreading operator:

$$\mathcal{I}_m(x_F) = \begin{cases} 1/h, & m = m_F = \text{round}\,(x_F/h) \\ 0, & \text{otherwise} \end{cases} \tag{40}$$

3.1.1. Iterative Conservative Finite Difference Scheme

Following the derivation in [8], a conservative, iterative finite difference scheme is constructed as

$$\rho\delta_{tt}u_m^n = \mathfrak{L}u_m^n + \frac{\delta_{t+}\phi_m^{n-1/2}}{\delta_{t\cdot}\eta_m^n} + \mathcal{I}_m\,(x_F)\,F^n \tag{41a}$$

$$\mathfrak{L}u_m^n = T_0\delta_{xx}u_m^n - EI\delta_{xxxx}u_m^n \tag{41b}$$

$$\eta_m^n = b_m - u_m^n \tag{41c}$$

Numerical boundary conditions, a discrete version of (34), are given as

$$u_m^n = \delta_{xx}u_m^n = 0 \qquad m = 0, M \tag{42}$$

The stability of the scheme can be inferred by energy analysis. Under unforced conditions, taking an inner product of (41a) with $\delta_{t\cdot}u_m^n$ gives the following energy balance

$$\delta_{t+}\left(\underbrace{\mathfrak{H}_k^{n-1/2} + \mathfrak{H}_p^{n-1/2} + \mathfrak{H}_c^{n-1/2}}_{\mathfrak{H}^{n-1/2}}\right) = 0 \tag{43a}$$

$$\mathfrak{H}_k^{n-1/2} = \frac{\rho\|\delta_{t-}u^n\|_{\mathbb{M}}^2}{2} \tag{43b}$$

$$\mathfrak{H}_p^{n-1/2} = \frac{T_0\left\langle \delta_{x+}u^n, \delta_{x+}u^{n-1}\right\rangle_{\mathbb{M}}}{2} + \frac{EI\left\langle \delta_{xx}u^n, \delta_{xx}u^{n-1}\right\rangle_{\overline{\mathbb{M}}}}{2} \tag{43c}$$

$$\mathfrak{H}_c^{n-1/2} = \left\langle 1, \phi^{n-1/2}\right\rangle_{\mathbb{M}} \tag{43d}$$

Because ϕ is non-negative, the total conserved energy will be non-negative under the standard stability condition for the stiff string, i.e. for

$$h^2 \geq \frac{T_0k^2 + \sqrt{T_0^2k^4 + 16EI\rho k^2}}{2\rho} \tag{44}$$

Under such condition, the bounds on the state read

$$0 \leq \|\delta_{t-}u^n\|_{\mathbb{M}} \leq \sqrt{2\mathfrak{H}^{1/2}/\rho} \tag{45}$$

Scheme (41a) can be cast in the following form, resembling the form for the lumped case of section 2.2.1

$$\underbrace{r_m - s_m + \frac{k^2}{\rho}\frac{\phi(-r_m + a_m) - \phi(a_m)}{r_m}}_{G(r_m)} = 0, \; m = 1, ..., M-1$$

where

$$s_m \triangleq 2u_m^n - 2u_m^{n-1} + \frac{k^2}{\rho}\mathfrak{L}u_m^n + \frac{k^2\mathcal{I}_m(x_F)}{\rho}F^n$$

$$r_m \triangleq u_m^{n+1} - u_m^{n-1}, \quad a_m \triangleq b_m - u_m^{n-1}$$

As this is an uncoupled system of nonlinear equations, the scheme can be shown to have a unique solution, as per the lumped system discussed in section 2.2.1. The solution to the system can be found using iterative solvers, such as Newton-Raphson—see [8, 5, 13].

3.1.2. Non-Iterative Conservative Finite Difference Scheme

A novel, non-iterative finite difference scheme arises as a discretisation of (29b). Hence

$$\rho\delta_{tt}u_m^n = \mathfrak{L}u_m^n + \left(\mu_{t+}\psi_m^{n-1/2}\right)\frac{\delta_{t+}\psi_m^{n-1/2}}{\delta_{t\cdot}\eta_m^n} + \mathcal{I}_m(x_F)F^n \tag{46}$$

where $\mathfrak{L}u_m^n$ and η_m^n are as per (41b) and (41c). The stability of the scheme can be inferred by energy analysis. Under unforced conditions, taking an inner product of (46) with $\delta_{t\cdot}u^n$ gives the same energy balance as (43a), where $\mathfrak{H}_k^{n-1/2}$, $\mathfrak{H}_p^{n-1/2}$ are as per (43b), (43c), and where

$$\mathfrak{H}_c^{n-1/2} = \frac{1}{2}\|\psi^{n-1/2}\|_{\mathbb{M}}^2 \tag{47a}$$

Hence, the total energy is non-negative under a choice of the grid spacing h as per (44), in which case the same bounds as (45) hold. As for the lumped case, described earlier in section 2.2.2, an extra equation relating u and ψ is needed. Again, one may conveniently use

$$\frac{\delta_{t+}\psi_m^{n-1/2}}{\delta_{t\cdot}\eta_m^n} = \psi'\Big|_{\eta=\eta_m^n} = \frac{\phi'}{\sqrt{2\phi}}\Big|_{\eta=\eta_m^n} \triangleq g_m^n \tag{48}$$

Making use of the following identity

$$\mu_{t+}\psi_m^{n-1/2} = \frac{k}{2}\delta_{t+}\psi_m^{n-1/2} + \psi_m^{n-1/2} \tag{49}$$

one can cast (46) in the following update form

$$A_m u_m^{n+1} = v_m \tag{50}$$

where

$$A_m = \frac{\rho}{k^2} + \frac{(g_m^n)^2}{4}$$

$$v_m = \frac{2\rho}{k^2}u_m^n - \frac{\rho}{k^2}u_m^{n-1} + \frac{(g_m^n)^2}{4}u_m^{n-1} - g_m^n\psi_m^{n-1/2} + \mathfrak{L}u_m^n$$

The whole system can be solved by a simple vector division. Once u_m^{n+1} is known, one may update $\psi_m^{n+1/2}$, using (48).

3.2. Non-Iterative Conservative Modal Scheme

A modal decomposition is readily available for the string described by (29a). The solution $u(x,t)$ is now expanded onto the eigenmodes for simply-supported boundary conditions, in the following way [17]

$$u(x,t) = \sum_{p=1}^{P} X_p(x) q_p(t) \tag{51}$$

The modal shapes and frequencies are given as

$$X_p(x) = \sin \frac{p\pi x}{L}, \quad \omega_p = \sqrt{\frac{p^2\pi^2}{L^2}\left(\frac{T_0}{\rho} + \frac{EI}{\rho}\frac{p^2\pi^2}{L^2}\right)} \tag{52}$$

Here, for practical purposes, the number of modes has been truncated to P (which is set by stability considerations, as per (61).) Inserting (51) into (29b), and taking an inner product with $X_p(x)$ results in $p = 1, .., P$ projected modal equations, of the form

$$\ddot{q}_p + \omega_p^2 q_p + \frac{X_p(x_F)}{\rho \|X_p\|^2} F(t) + \frac{\langle \psi g, X_p \rangle_{\mathcal{D}}}{\rho \|X_p\|^2} = 0 \tag{53}$$

where

$$g = \frac{\partial_t \psi}{\partial_t \eta}, \quad \eta = b - \sum_{p=1}^{P} X_p(x) q_p(t) \tag{54}$$

It is possible to define a modal energy conservation law, by inserting the modal expansion above into (33b), and by using the fact that $\|X_p\|^2 = \frac{L}{2}\ \forall p$. Hence

$$\frac{d}{dt}\left[\underbrace{\frac{\rho L}{2}\sum_{p=1}^{P}\left(\frac{(\dot{q}_p)^2}{2} + \frac{(\omega_p q_p)^2}{2}\right) + \frac{\|\psi\|_{\mathcal{D}}^2}{2}}_{H(t)}\right] = 0 \tag{55}$$

From the above, it is possible to extract a bound on a single mode p, as

$$0 \leq |\partial_t q_p| \leq \sqrt{4H_0/\rho L} \tag{56}$$

Discretisation of (53) and (54) follows as

$$\delta_{tt} q_p^n + \omega_p^2 q_p^n + \frac{X_p(x_F)}{\rho \|X_p\|^2} F^n + \frac{\left\langle (\mu_{t+}\psi^{n-1/2}) g^n, X_p \right\rangle_{\mathcal{D}}}{\rho \|X_p\|^2} = 0 \tag{57}$$

$$\frac{\delta_{t+}\psi^{n-1/2}}{\delta_{t\cdot}\eta^n} = g^n \triangleq \psi' \Big|_{\eta=\eta^n} \tag{58}$$

Making use of identity (27), one may rewrite the first equation above as

$$\delta_{tt} q_p^n + Q_p + \omega_p^2 q_p^n + \frac{X_p(x_F)}{\rho \|X_p\|^2} F^n + \frac{\left\langle \psi^{n-1/2} g^n, X_p \right\rangle_{\mathcal{D}}}{\rho \|X_p\|^2} = 0 \tag{59}$$

where Q_p is a coupling term, i.e.

$$Q_p = \frac{k}{2\rho \|X_p\|^2} \left\langle (g^n)^2 \delta_{t\cdot}\eta^n, X_p \right\rangle_{\mathcal{D}} \tag{60}$$

The modal coordinates q_p can then be solved using (59), which is in the form of a non-sparse linear system with non-sparse elements given by Q_p. Notice that the resulting non-sparse matrix is in the form of a rank-one perturbation, resolvable very efficiently using the Sherman-Morrison formula [18]. One can then update ψ using (58). The stability of the scheme can once again be understood in terms of its energy-preserving properties. For this scheme, in fact, energy conservation reads

$$\delta_{t+}\left[\underbrace{\frac{\rho L}{2}\sum_{p=1}^{P}\left(\frac{(\delta_{t-}q_p^n)^2}{2} + \frac{\omega_p^2 q_p^n q_p^{n-1}}{2}\right) + \frac{\|\psi^{n-1/2}\|_{\mathcal{D}}^2}{2}}_{\mathfrak{H}^{n-1/2}}\right] = 0$$

and hence, remembering (21), the largest eigenfrequency allowed for this scheme is such that

$$\omega_P < 2 f_s \tag{61}$$

Notice that the contribution of a single mode p to the total energy is non-negative. Hence, boundedness can be stated mode by mode, as

$$0 \leq |\delta_{t-} q_p^n| \leq \sqrt{4\mathfrak{H}^{1/2}/\rho L} \tag{62}$$

3.3. Numerical Examples and Discussion

The three schemes described in the previous sections are now compared in cases of interest in musical acoustics. A first experiment takes into account the case of a point barrier, located at the centre of the domain. Fig. 4 shows a few snapshots of the dynamics of the string, before, during and after contact with the barrier. The three schemes yield consistent solutions, although some differences are also observed.

As for the lumped case of section 2.3, a closer look at the energy components can be revealing. Fig. 5 shows the kinetic, potential and collision energies of the three schemes over time. The non-iterative schemes tend to transform the excess kinetic energy during a collision into extra collision energy, so that bounds (45) are indeed verified. This allows to keep the scheme stable, but it also results in a deterioration of the kinetic and potential energy components. This is particularly evident for the non-iterative finite difference scheme, whereas the modal scheme is somewhat better behaved: this may be a reflection of the modal boundedness property (62). Notice, however, that the total energy of the three schemes is conserved after the forcing vanishes, with the three schemes having the same total energy overall, as expected. Of course, one may increase the sample rate, and observe convergence of the three schemes toward a unique solution, which therefore can be identified as the solution to the original problem. The energy components of Fig. 6 are much more consistent, and the recorded outputs shown in Fig. 7 seem to have converged. Certainly, the solution computed via the classic iterative scheme is characterised by a faster convergence rate. In other words, for the same sample rate, the classic iterative scheme yields a solution closer to the converged solution than the non-iterative schemes. On the other hand, the non-iterative solvers are extremely efficient in this case: the non-iterative finite difference scheme is fully explicit, a rarity in the realm of nonlinear problems. One may exploit this feature in a number of ways, most noticeably using parallel instructions on CPUs and GPUs, alleviating the extra computational burden coming from oversampling. Basic experiments in Matlab show significant speedups: for the experiment of Fig. 8, the new non-iterative finite difference scheme with an oversampling factor

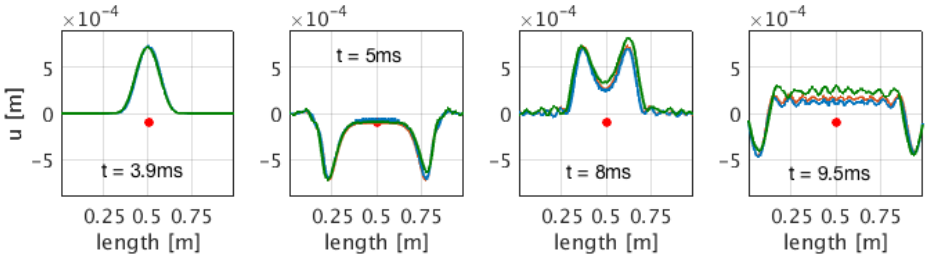

Figure 4: Snapshots of a simulated string colliding against a point barrier. For all panels, the red line is the benchmark (iterative) scheme, the blue line is the non-iterative finite difference method, and the green line is the modal non-iterative method. The point barrier has $K = 5 \cdot 10^6$, $\alpha = 1.4$, $b = 10^{-4}$m and is located at $x = 0.5$m. The string has $L = 1$m, $\rho = 0.063$kg/m, radius $r = 5 \cdot 10^{-4}$m, $T_0 = 500$N, $E = 2 \cdot 10^{11}$Pa. The string is set into motion by a raised cosine input force, with $F_0 = 10$N, and $t_{wid} = 1$ms. The sample rate for this simulation is $f_s = 44100$Hz.

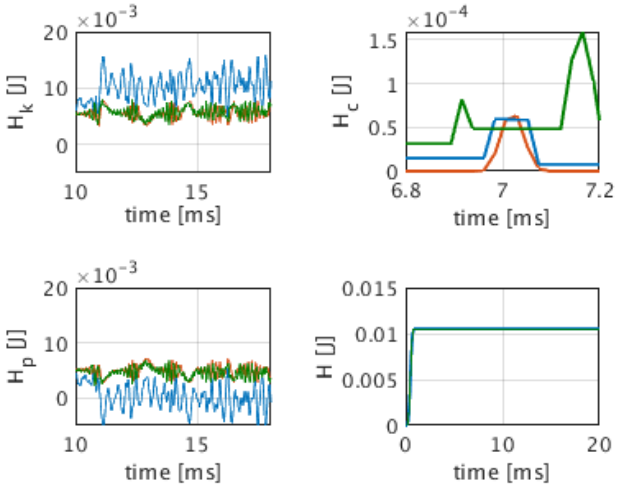

Figure 5: Energy components for the simulations of Fig. 4, where $\mathfrak{H}_k$ stands is the kinetic energy, $\mathfrak{H}_c$ is the collision energy, $\mathfrak{H}_p$ is the potential energy, and $\mathfrak{H}$ is total energy. Colour scheme as Fig. 4

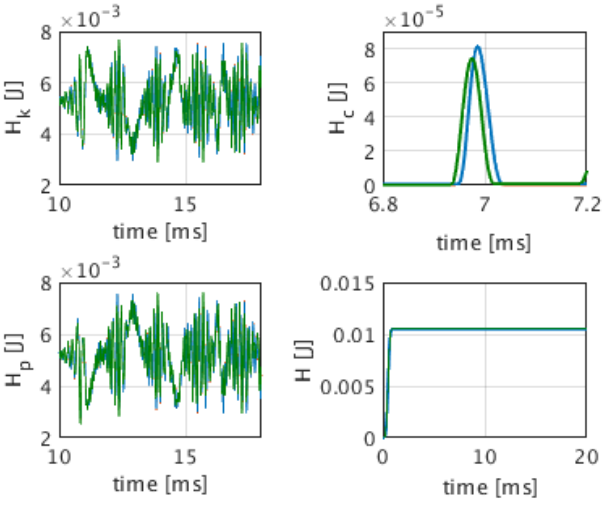

Figure 6: Same as Fig. 5, but with $f_s = 5 \cdot 44100$Hz.

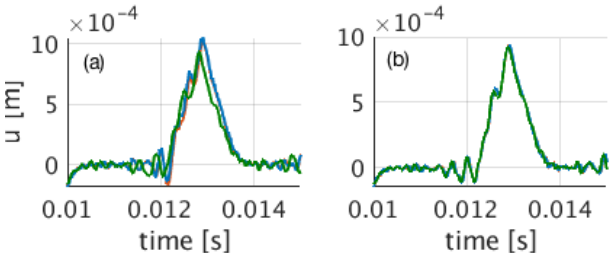

Figure 7: Recorded output at $x_o = 0.9L$. (a): $f_s = 44100$Hz, (b): $f_s = 5 \cdot 44100$Hz. All other parameters as per Fig. 4

of 5 is faster than the iterative finite difference scheme at audio rate (using a fixed number of 20 iterations per collision). A more consistent comparison, in C++, is drawn in the companion paper [14], highlighting time gains of up to an order of magnitude. Assessing the efficiency of the modal non-iterative scheme requires some care. For collisions, modal methods have been successfully implemented in the past. In [12], a non-iterative modal scheme is given, for $\alpha = 1$. In [11], all values of α are allowed, and a spatial grid is used along with an iterative procedure . The novel non-iterative modal schemes presented here can be implemented efficiently, for all values of α, using the Sherman-Morrison formula [18]. Whether or not the non-iterative modal scheme are "faster" than the non-iterative finite difference schemes depends on a number of factors, such as number of modes, sample rate, and number of barrier points. In general, for smaller sizes, the modes can be extremely fast, but in the case of many barrier points, such as the example of Fig. 8, the modal scheme requires the calculation of as many reduced sums, and this has a significant impact of the overall efficiency. The relative efficiency of the schemes proposed will not be discussed further here, but it certainly deserves a closer investigation. As a concluding experiment, the three schemes are used to solve the case of a string colliding against a fairly rigid bent distributed obstacle, as per Fig. 8. This is similar to what happens in tanpuras, and other string instruments, although the simulation parameters are here only meant for illustrative purposes. The three schemes yield the consistent solutions after multiple collisions.

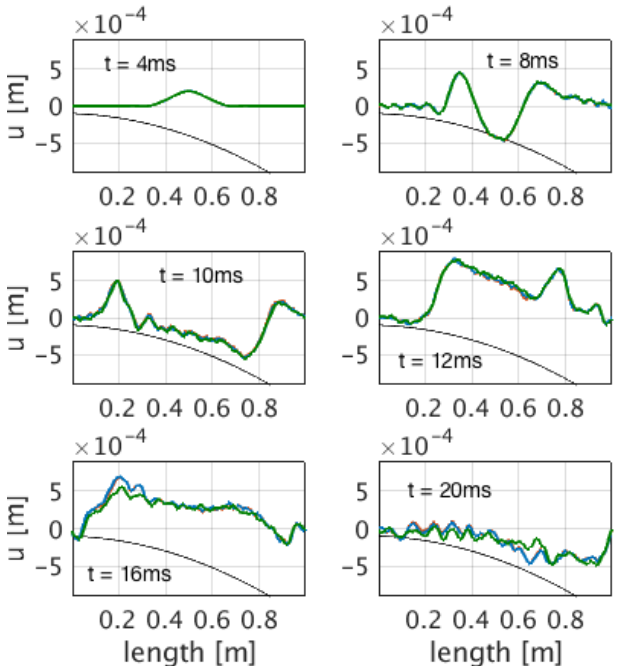

Figure 8: Snapshots of a simulated string colliding against a distributed barrier. For all panels, the red line is the benchmark (iterative) scheme, the blue line is the non-iterative finite difference methods, and the green line is the modal non-iterative method. The barrier has $K = 5 \cdot 10^6$, $\alpha = 1.4$, $b = -10^{-4} - 10^{-4}x - 10^{-3}x^2$. For the modal scheme, the barrier was created by placing point obstacles at locations corresponding to the grid points of the finite difference schemes. The string has $L = 1$m, $\rho = 0.063$kg/m, $r = 5 \cdot 10^{-4}$m, $T_0 = 500$N, $E = 2 \cdot 10^{11}$Pa. The string is set into motion by a raised cosine input force, with $F_0 = 10$N, and $t_{wid} = 1$ms. The sample rate for this simulation is $f_s = 5 \cdot 44100$Hz.

4. CONCLUSIONS

In this work, a novel family of schemes was presented for the solution of collisions in musical acoustics. The case of collisions represents but one of a very large class of nonlinear problems that can be treated within the illustrated framework. The new schemes are non-iterative, and they require at most the solution of a linear system. In particular, for the fully distributed case, a finite-difference non-iterative scheme and a modal non-iterative scheme have been given, with the former being completely explicit. Stability and convergence of the proposed methods have been demonstrated formally, using energy arguments, and via numerical experiments. The new schemes have a slower convergence rate than the benchmark iterative schemes obtained via implicit methods, but they are also much more efficient. Basic experiments in Matlab show that the non-iterative oversampled schemes can be faster than the benchmark iterative schemes run at audio rate. Oversampling was employed here as a corrective measure, but different strategies could and should be investigated in future works.

5. ACKNOWLEDGMENTS

The first author wishes to thank the Leverhulme Trust, who is supporting his research with an Early Career Fellowship.

6. REFERENCES

[1] A. Falaize and T. Hélie, "Passive Guaranteed Simulation of Analog Audio Circuits: A Port-Hamiltonian Approach," *Appl. Sci.*, vol. 6, pp. 273 – 273, 2016.

[2] A. Falaize, *Modélisation, simulation, génération de code et correction de systèmes multi-physiques audios: Approche par réseau de composants et formulation Hamiltonienne À Ports*, Ph.D. thesis, Université Pierre et Marie Curie, Paris, July 2016.

[3] N. Lopes, T. Hélie, and A. Falaize, "Explicit second-order accurate method for the passive guaranteed simulation of port-hamiltonian systems," in *Proc. 5th IFAC 2015*, Lyon, France, July 2015.

[4] X. Yang, "Linear and unconditionally energy stable schemes for the binary fluid-surfactant phase field model," *Comp. Methods Appl. Mech. Eng.*, vol. 318, pp. 1005–1029, 2017.

[5] M. Ducceschi and S. Bilbao, "Modelling collisions of nonlinear strings against rigid barriers: Conservative finite difference schemes with application to sound synthesis," in *Proc. Int. Conf. On Acoust. (ICA 2016)*, Buenos Aires, Argentina, September 2016.

[6] M. Ducceschi, "A numerical scheme for various nonlinear forces, including collisions, which does not require an interative root finder," in *Proc. Int. Conf. On Dig. Audio Eff. (DAFx 2017)*, Edinburgh, UK, September 2017.

[7] V. Chatziioannou, S. Schmutzhard, and S. Bilbao, "On iterative solutions for numerical collision models," in *Proc. Int. Conf. On Dig. Audio Eff. (DAFx 2017)*, Edinburgh, UK, September 2017.

[8] S. Bilbao, A. Torin, and V. Chatziioannou, "Numerical modeling of collisions in musical instruments," *Acta Acust. United Ac.*, vol. 101, pp. 155 – 173, 2015.

[9] V. Chatziioannou and M. van Walstijn, "Energy conserving schemes for the simulation of musical instrument contact dynamics," *J. Sound Vib.*, vol. 339, pp. 262 – 279, 2015.

[10] C. Issanchou, V. Acary, F. Pérignon, C. Touzé, and J-L. Le Carrou, "Nonsmooth contact dynamics for the numerical simulation of collisions in musical string instruments," *J. Acoust. Soc. Am.*, vol. 143, no. 5, pp. 3195, 2018.

[11] C. Issanchou, J.-L. Le Carrou, C. Touzé, B. Fabre, and O. Doaré, "String/frets contacts in the electric bass sound: Simulations and experiments," *Appl. Acoust.*, vol. 129, pp. 217 – 228, 2018.

[12] M. van Walstijn, J. Bridges, and S. Mehes, "A real-time synthesis oriented tanpura model," in *Proc. Int. Conf. On Dig. Audio Eff. (DAFx 2016)*, Brno, Czech Republic, September 2016.

[13] V. Chatziioannou and M. van Walstijn, "An energy conserving finite difference scheme for simulation of collisions," in *Proc. SMAC/SMC 2013*, Stockholm, Sweden, August 2013.

[14] S. Bilbao, M. Ducceschi, and C. Webb, "Large-scale real-time modular physical modeling sound synthesis," in *Proc. Int. Conf. On Dig. Audio Eff. (DAFx 2019)*, Birmingham, UK, September 2019.

[15] K.H. Hunt and F.R.E. Crossley, "Coefficient of restitution interpreted as damping in vibroimpact," *J. Appl. Mech.*, vol. 42, no. 52, pp. 440–445, 1975.

[16] S. Bilbao, *Numerical Sound Synthesis: Finite Difference Schemes and Simulation in Musical Acoustics*, Wiley, Chichester, UK, 2009.

[17] M. Ducceschi and S. Bilbao, "Linear stiff string vibrations in musical acoustics: Assessment and comparison of models," *J. Acoust. Soc. Am.*, vol. 140, no. 4, pp. 2445–2454, 2016.

[18] J. Sherman and W. J. Morrison, "Adjustment of an inverse matrix corresponding to a change in one element of a given matrix," *Ann. Math. Stat.*, vol. 21, pp. 124–127, 1950.